# NUMERICAL STUDY CONCERNING THERMAL RESPONSES OF NANOFILMS UNDER THE THERMOMASS THEORY

**R. S. M. Freitas,**
**C. S. Stampa,**
**D. C. Lobão,**
**and G. B. Alvarez**

[a]Universidade Federal Fluminense
PPG-Modelagem Computacional em Ciência e Tecnologia
Escola de Engenharia Industrial Metalúrgica de Volta Redonda
Av. dos Trabalhadores No 420
Vila Santa Cecília, Volta Redonda, RJ, Brasil
CEP: 27225-125
rodolfosmfreitas@gmail.com

Received: December 02, 2015
Revised: February 08, 2016
Accepted: April 01, 2016

## ABSTRACT

The Thermomass theory is based on the relationship mass-energy of Einstein, i.e., the heat has mass-energy duality, behaving as energy in processes where its conversion occurs in another form of energy, and behaving as mass in heat transfer processes. The mathematical model stablished by the Thermomass model falls within the class of problems called models non-Fourier heat conduction. The present work aims to analyze the thermal responses provided by Thermomass theory of nanofilms submitted to a very fast heating process using two different heat sources (laser pulses). During the process of analysis, the equations are written in conservation law, put into dimensionless form and discretized in the way that a high-order TVD scheme is used on to provide accurate and reliable numerical simulations for obtaining the thermal responses predicted by the Thermomass model. The results show that the Thermomass theory predicted a heterogeneous temperature distribution with elevated temperature peaks. The thermal responses obtained from this model may prevent the thermal damage caused by technologies of the processing and manufacturing of elements based on high-power laser applications.

**Keywords**: hyperbolic heat conduction in nanofilms, non-Fourier heat conduction, thermomass theory, TVD scheme

## NOMENCLATURE

| | |
|---|---|
| $c$ | speed of light, m/s |
| $C$ | specific heat, J/(kg.K) |
| $f$ | resistance force, N/m$^3$ |
| $H$ | nanofilm length, m |
| $k$ | thermal conductivity, W/(m.K) |
| $L$ | nanofilm width, m |
| $\dot{m}$ | rate of mass flow, kg/(m$^2$.s) |
| $p$ | pressure, N/m$^2$ |
| $q$ | heat flux, W/m$^2$ |
| $t$ | time, s |
| $T$ | absolute temperature, K |
| $u$ | velocity of the thermomass gas flow, m/s |
| $x, y$ | coordinates, m |
| $Z_T$ | dimensionless characteristic time |

### Greek symbols

| | |
|---|---|
| $\alpha$ | thermal diffusivity, m$^2$/s |
| $\beta$ | proportionality coefficient for resistance |
| $\gamma$ | Grüneisen constant |
| $\kappa$ | ratio of specific heats |
| $\rho$ | density, kg/m$^3$ |
| $\tau$ | characteristic time, s |
| $\varphi$ | parameter for state equation, Eq. (4) |

### Subscripts and Superscripts

| | |
|---|---|
| *0* | initial condition |
| * | dimensionless variables |
| *A* | laser intensity |
| *Cos* | Cosseinodal pulse function |
| *d* | pulse duration |
| *G* | Gaussian pulse function |
| *Th* | thermomass gas |

## INTRODUCTION

Short pulse lasers with pulse duration of the order of femto/picoseconds have been studied extensively over the past two decades. The heating by laser pulse is becoming an important tool for studying the thermal properties in nanofilms (Miklos and Lorincz, 1988; Eesley, 1990). In addition, new technologies based in heating by laser are developing rapidly due to increased availability of high-power lasers. Therefore, understanding the heat conduction processes under these conditions is of great importance for the evaluation of performance and improvement of these technologies.

The first studies on heat conduction were performed by J. Fourier (Fourier, 1878) in 1822. From experimental results Fourier formulated a constitutive equation, which was called Fourier's law for the heat conduction. This equation states that the rate of heat transfer by conduction is proportional to

the area of the cross section, perpendicular to its direction of propagation, the difference between the highest and the lowest temperature involved, and is inversely proportional to the distance between these temperatures. The differential form of the Fourier's law of heat conduction is

$$q = -k\nabla T \quad (1)$$

where $q$ is the local heat flux, $k$ is the thermal conductivity of the medium and $T$ is the local temperature. Fourier's law is simple within mathematics and has been extensively used, although it is only an empirical relationship. However, for the transient heat conduction process the Fourier's law leads to an unphysical infinite heat propagation speed within the continuum field (Fichera, 1992). The infinite speed of propagation of heat in the medium is physically unrealistic. However, it is found that this law returns accurate answers of the heat conduction in most engineering applications. The limitation imposed by Fourier's law is not important except in extremely small time and length scales (Chen, 2000). Recently, the heat conduction schemes in function of time and length scales were outlined by (Escobar et al., 2006). In their work, Escobar et al. verified that the Fourier's law is valid only when the characteristic length of the medium is much larger than the mean free path of heat carriers. Fourier's law is also valid when the process time scale is much larger than the time required for thermodynamic equilibrium in the medium after suffering a thermal disturbance.

With the rise of nanotechnology and consequently the technologies of the processing and manufacturing of elements based on heating by short-pulse lasers, the need is stablished to investigate the heat conduction process in nanoscale. From theoretical and experimental results, produced by (Yang et al., 2010) and (Chang et al., 2008), respectively, it was verified that Fourier's law when applied to nanoscale obtains unsatisfactory results. Thus, it becomes invalid for analysis of heat transfer by conduction in nanomaterials.

In order to overcome the contradiction imposed by Fourier's law, several theories have been developed to describe the conduction heat transfer process (Cattaneo, 1948; Vernotte, 1958; Qiu and Tien, 1992; Tzou, 1995; Guo, 2006). Its mathematical models are often called non-Fourier heat conduction models. Some studies have been performed using non-Fourier heat conduction models to analyze the heat conduction in metallic nanofilms heated by an ultrafast laser pulse (Zhou and Ma, 2011; Wang et al. 2011).

Besides the models that use the theory of the continuum there are also models created using quantum mechanics. Recent studies were performed using the Boltzmann transport equation to investigate the heat conduction in silicon nanowires and nanofilms (Terris et al., 2007; Zou et al., 2014; Hua and Cao, 2014).

Recently, Guo and Huo (Guo and Huo, 2010) analyzed the transient heat conduction process into a silicon nanofilm heated by a heat pulse using the Thermomass theory. For the case of a material with a high thermal conductivity, Wang et al. (Wang et al., 2010) analyzed the transient heat conduction process and they found that the other non-Fourier conduction models presented unphysical responses to the temperature distribution, similarly reported in (Bai and Lavine, 1995; Korner and Bergmann, 1998). However, the Thermomass model results in a reasonable response of the temperature distribution. For the steady heat conduction process, (Guo et al., 2011; Wang et al., 2012) predicted the thermal conductivity of nanomaterials, as nanofilms, nanotubes and nanowires.

The present work aims to analyze the thermal responses predicted by Thermomass theory of nanofilms submitted to a heating process using two different heat sources (laser pulses). For the numerical resolution, the governing equations are written in the conservation law form, discretized and an explicit TVD (Total Variation Diminishing) scheme is applied (Yee, 1987; Lobão, 1992; Lobão, 2002).

## MATHEMATICAL MODELLING

In this article, numerical simulations are conducted to evaluate the process of non-Fourier heat conduction in a nanofilm due to the presence of high intensity heat fluxes caused from high intensity laser pulses and due to the extremely small cross sections areas.

Figure 1, in the part (a), shows an actual longitudinal section of the nanofilm of width $L$, where the length of it is considered much larger than its width. It is considered that the heat pulse is applied uniformly along of left boundary and the right boundary of the same is attached in a medium whose thermal conductivity is much smaller than the nanofilm. Part (b) of Fig. 1 represents the physical model used to analyze non-Fourier heat conduction under Thermomass theory. The length $H$ in the physical model is a fictitious dimension once the heat pulse is applied uniformly along the entire left boundary of the nanofilm. Thus, the heat propagates exclusively from the left to the right boundary, i.e., in the $x$ direction.

The method used to evaluate the transient thermal responses in nanofilms is through the application of two different laser pulses to the left boundary, which results into two specific time-varying heat fluxes. These heat fluxes have equal maximum intensity and equal application time. However, their temporal intensity variations are different.

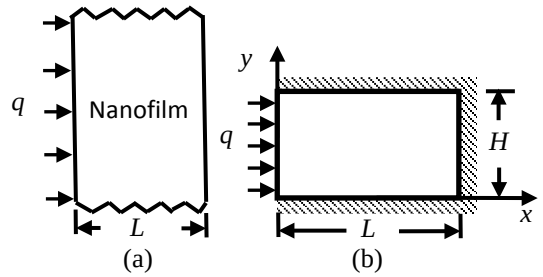


Figure 1. Schematic diagram: (a) Actual longitudinal section of the nanofilm; (b) Physical model.

In this paper, the Thermomass theory is used to investigate the non-Fourier heat conduction in nanofilms. The Thermomass theory based on the relationship mass-energy of Einstein (Einstein et al., 1952), i.e., the heat has mass-energy duality, behaving as energy in processes where its conversion occurs in another form of energy, and behaving as mass in heat transfer processes. In most cases of thermophysics, the Thermomass is generally very small, about $10^{-16}$ kg of Joule (J) of heat, and the inertia effects can be neglected. Thus, the heat conduction can be treated as a diffusion process. However, the inertial effects shouldn't be ignored for the ultrafast heating processes or a process having a high rate of heat transfer.

The Thermomass theory considers that the heat is carried by thermons. The thermon is defined as the unity of a quasi-particle carrying thermal energy (Wang et al., 2010). Considering that the thermons are much smaller than the material particles which constitute the medium and in a material volume contain a sufficient number of thermons such that it is possible to get the main parameters that adequately describe the medium. It is assumed that a collection of thermons forms a Thermomass gas, where this is considered as a continuum medium. Thus, the process of heat conduction in a solid driven by a temperature gradient can be understood as a Thermomass gas which flows through the molecules, atoms, or reticles of the medium just as a real gas flows through a porous medium. Therefore, the transport process can be described by Newtonian mechanics.

In order to analyze the Thermomass gas movement is necessary initially obtain the state equation that governs the medium. The equation of state for thermomass gas in the ideal gas is given by (Wang et al., 2010)

$$p_{Th} = \kappa \rho_{Th} CT \tag{2}$$

where $p_{Th}$ is the Thermomass pressure, $\rho_{Th}$ is the density of Thermomass gas, $T$ the local temperature, $\kappa$ denotes the ratio of specific heats and $C$ is the specific heat of medium.

In dielectric materials, the heat conduction occurs due to vibration of atoms. The atoms are connected by interatomic forces of interaction, where the minimum interatomic potential defines the equilibrium positions of the atoms.

The motion of each atom is restricted by its neighboring atoms due to the interatomic potential. A simplified view of the interatomic interactions in a crystalline solid can be represented by a mass-spring system. In this system, the vibration of any atom can propagate and cause the vibration of the entire system, thus, creating elastic waves in the system. If one side of a solid is heated, the atoms near to the hot side will have larger amplitudes of vibration, which will be felt by atoms in the opposite side of the medium through the propagation and interaction of the elastic waves.

The minimum energy of a quantized elastic wave is called a phonon (Chen, 2005). A phonon at a particular frequency and wavelength is a wave that extends through the entire crystalline solid. The superposition of phonons having multiple vibration frequencies in a solid forms wave packets, which these packets can be considered as particles as long as they are much smaller than the size of the crystal. Therefore, heat in a dielectric is conducted by a phonon gas similar to an ideal gas.

For the case of dielectric solids, (Guo and Huo, 2010; Wang et al., 2010) developed an equation of state of the phonon gas. The equation of state for the phonon gas based on the Debye state equation is given by

$$p_{Th} = \gamma \rho_{Th} CT \tag{3}$$

where $\gamma$ is the Grüneisen constant.

It is verified that the state equation for the phonon gas is very similar to the state equation for the ideal gas, except for the proportional parameters, $\gamma$ and $\kappa$. Therefore, can be established a general state equation for the Thermomass gas as

$$p_{Th} = \varphi \rho_{Th} CT \tag{4}$$

where $\varphi$ is a proportional parameter, whose value differs for different states of the medium.

Concerning the determination of the density of the Thermomass gas, it can be obtained as a function of medium density

$$\rho_{Th} = \frac{\rho CT}{c^2}, \tag{5}$$

where $\rho$ is the density of medium and $c$ is the speed of light.

To get the governing equations of Thermomass gas flow, it is initially necessary to define the velocity of the Thermomass gas flow. When there is a temperature gradient in a medium, the heat flows from the highest region to the lowest temperature

region. This indicates that the Thermomass gas flows with a determined velocity. Based on the concept of Thermomass, the mass flow rate of the Thermomass gas can be calculated as

$$\dot{m}_{Th} = \rho_{Th} u_{Th}\,, \tag{6}$$

where $u_{Th}$ is the velocity of the Thermomass gas flow. From Einstein's mass-energy relation $\dot{m}_{Th}=q/c^2$, where $q$ is heat flux. Thus, it follows that the flow velocity of the Thermomass gas is given by

$$u_{Th} = \frac{q}{\rho C T} \tag{7}$$

Equation (7) indicates that the flow velocity of the Thermomass gas is equivalent to the transport velocity of the heat flux, in which this is calculated by dividing the heat flux by thermal energy per volume unit. Therefore, obtaining the flow velocity can investigate the heat conduction process using the governing equations for the Thermomass gas movement, as is realized in fluid dynamics.

It is considered the Thermomass gas flow as the flow of a compressible fluid in a porous medium, where this medium is considered homogenous and isotropic, with constant physical proprieties. It is assumed that Thermomass gas flow is driven by a temperature gradient in a medium without internal heat sources. Thus, applying the Newtonian mechanics in order to analyze the Thermomass gas transport, it follows that the equations that govern the Thermomass gas transport are given by

$$\frac{\partial \rho_{Th}}{\partial t} + \nabla \cdot \left(\rho_{Th} u_{Th}\right) = 0\,. \tag{8}$$

$$\rho_{Th} \frac{D u_{Th}}{D t} + \nabla p_{Th} + f_{Th} = 0\,, \tag{9}$$

where $D/Dt$ represents the total derivative and $f_{Th}$ is the resistance force to the Thermomass flow per volume unit.

Equations (8) and (9) describe the Thermomass gas transport in continuum materials. The introduction of the resistance force term, rather than to use the viscosity terms in the momentum equation is due to the difficulty in determining the viscosity of the Thermomass gas for specific materials. A second difficulty is related to describe how the interaction between Thermomass gas and the material particles of the medium occurs.

Based on the Thermomass theory is possible to establish a set of equations which govern the heat conduction in a continuum medium. Introducing the Eqs (3), (5) and (7) into Eqs. (8) and (9) obtains the governing equations the heat conduction. For the one-dimensional case Eqs. (8) - (9), can be simplified as

$$\rho C \frac{\partial T}{\partial t} + \frac{\partial q}{\partial x} = 0 \tag{10}$$

$$\frac{\partial q}{\partial t} - \frac{q}{T}\frac{\partial T}{\partial t} + \frac{q}{\rho C T}\frac{\partial q}{\partial x} - \frac{q^2}{\rho C T^2}\frac{\partial T}{\partial x} + \\ + 2\varphi\rho C^2 T \frac{\partial T}{\partial x} + f_{Th} c^2 = 0\,, \tag{11}$$

where the first four terms of Eq. (11) are related to the total derivative of the Thermomass gas velocity, the same refer to the inertial effects. The fifth term is associated with the pressure effect of the Thermomass gas. Finally, the sixth term represents the resistance effects of the Thermomass gas flow.

When the flow velocity of the Thermomass gas is very small, the resistance force is proportional to the flow velocity (Wang et al., 2010), being expressed

$$f_{Th} = \beta u_{Th}\,, \tag{12}$$

where $\beta$ is a parameter to be determined. Assuming that Eq. (11) has to be consistent with Fourier's law as long as the inertial terms are neglected. The value of the parameter $\beta$ can determined as

$$\beta = \frac{2\varphi\rho^2 C^3 T^2}{c^2 k}\,, \tag{13}$$

where $k$ is the medium thermal conductivity.

Therefore, the general heat conduction equation considering a linear resistance force is given by

$$\tau_{Th}\left(\frac{\partial q}{\partial t} + \frac{q}{\rho C T}\frac{\partial q}{\partial x}\right) - \tau_{Th}\frac{q}{T}\left(\frac{\partial T}{\partial t} + \frac{q}{\rho C T}\frac{\partial T}{\partial x}\right) + \\ + k\frac{\partial T}{\partial x} + q = 0\,, \tag{14}$$

where $\tau_{Th}$ is the characteristic time. The same represents the time delay between the Thermomass gas flow and its driven force. The characteristic time is determined by the physical properties and the local temperature of the medium

$$\tau_{Th} = \frac{\alpha}{2\varphi C T}\,, \tag{15}$$

where $\alpha$ is the thermal diffusivity.

By introducing Eq. (10) into Eq. (14) the final form of the governing equations for one-dimensional heat conduction is obtained. To complete the mathematical formulation, the following initial and boundary conditions are then specified for the physical domain,

$$\frac{\partial T}{\partial t}+\frac{1}{\rho C}\frac{\partial q}{\partial x}=0 \tag{16}$$

$$\frac{\partial q}{\partial t}+2\frac{q}{\rho C T}\frac{\partial q}{\partial x}-\frac{1}{\rho C}\left(\frac{q}{T}\right)^2\frac{\partial T}{\partial x}+ +\frac{k}{\tau_{Th}}\frac{\partial T}{\partial x}+\frac{q}{\tau_{Th}}=0, \tag{17}$$

Equations (16)-(17) represent the mathematical model to be utilized in the present work. This system of equations is coupled and must be solved simultaneously with the application of an appropriate numerical method.

## NUMERICAL METHOD AND VALIDATION

To eliminate the scale order problems, Eqs. (16) and (17) are cast in the dimensionless form. By introducing the following dimensionless quantities:

$$t^*=\frac{t}{\left(L^2/\alpha\right)},\quad x^*=\frac{x}{L},\quad T^*=\frac{T}{T_0},\quad q^*=\frac{q}{\left(\rho\alpha C T_0/L\right)},\quad Z_{Th}=\frac{\alpha\tau_{Th}}{L^2}, \tag{18}$$

where $T_0$ is the initial temperature of the medium.

Equations (16) and (17) can be rewritten in the dimensionless conservation law form as

$$\frac{\partial E}{\partial t^*}+B\frac{\partial F}{\partial x^*}+H=0, \tag{19}$$

where

$$E=\begin{bmatrix}T^*\\ q^*\end{bmatrix},\quad F=\begin{bmatrix}q^*\\ T^*\end{bmatrix},$$

$$B=\begin{bmatrix}1 & 0\\ 2\dfrac{q^*}{T^*} & \left(\dfrac{1}{Z_{Th}}-\left(\dfrac{q^*}{T^*}\right)^2\right)\end{bmatrix},\quad H=\begin{bmatrix}0\\ \dfrac{q^*}{Z_{Th}}\end{bmatrix}. \tag{20}$$

According to the physical model, Fig. 1 (b), the initial-boundary conditions are given as follows

$$0\le x^*\le 1 \text{ and } t^*=0: T^*=1 \tag{21}$$

$$x^*=0 \text{ and } t^*>0: q^*=q^*\left(t^*\right) \tag{22}$$

$$x^*=1 \text{ and } t^*>0: \frac{\partial T^*}{\partial x^*}=0. \tag{23}$$

Eq. (19) can be solved by a high-order TVD scheme with *mimmod* limiter function, the detail of which can be found in (Yee, 1987; Lobão, 1992; Lobão, 2002.).

Before establishing the TVD scheme for obtaining the thermal responses predicted by the Thermomass model, should be testify the validity of this adopted scheme in solving the governing equations. The one-dimensional transient heat conduction in a silicon nanofilm reported by Wang et al. (Wang et al., 2010) was taken for the validation of the numerical method used in this paper. Wang et al. considered the temperature response in a silicon nanofilm heated from a heat flux pulse in the left side. The right side of the nanofilm is assumed thermally insulated. The nanofilm is 0.2 μm thick and the initial temperature is 300 K. The heat flux pulse on the left side can be expressed as

$$q(0,t)=\begin{cases}q_A\times\dfrac{1}{2}\left(1-\cos\left(\dfrac{2\pi t}{t_d}\right)\right), & t<t_d,\\ 0, & t\ge t_d\end{cases} \tag{24}$$

where $q_A$=5x10$^{11}$ W/m$^2$ and $t_d$=20 ps. The physical properties of the silicon nanofilm are assumed constant, being the density $\rho$=2330 kg/m$^3$, the thermal conductivity $k$=163 W/m K, the specific heat $C$=657 J/kg K and the Gruneisen constant $\gamma$=1.96.

Initially, the results are obtained in the dimensionless form and, after, applies an inverse transformation, i.e., from the results of the dimensionless variables are obtained the results of the interest variables in the dimensional form. This transformation is performed according to Eq. (18).

Figure 2 presents the comparison between the spatial temperature distributions at $t$= 20 ps predicted by the Thermomass model using the present numerical scheme and the numerical solution reported by Wang et al. (Wang et al., 2010). From Fig. 2, it can be easily seen that the result obtained from TVD scheme presented very good agreement with that obtained by Wang et al., which justifies the credibility of the TVD scheme in solving the Thermomass heat conduction equation.

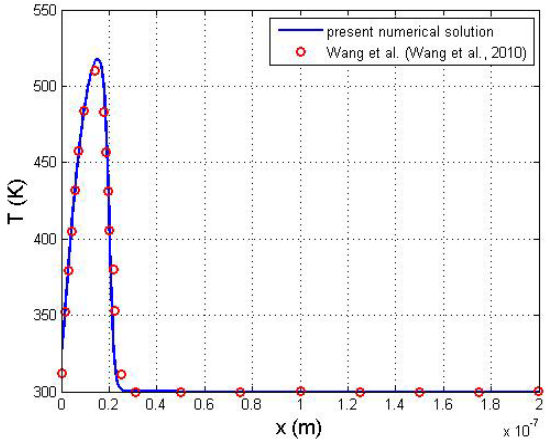


Figure 2. Comparison between the spatial temperature distributions at t= 20 ps obtained by present numerical scheme and the numerical solution reported by Wang et al. (Wang et al., 2010).

## NUMERICAL RESULTS AND DISCUSSIONS

For the numerical resolution of the governing equations, the explicit TVD (Total Variation Diminishing) method has been used (Yee, 1987; Lobão, 1992). Equation (19) was discretized using central difference for spatial discretization and forward difference for temporal discretization. After tests with different meshes and time steps, a fixed and regular mesh with 1000 grid points and with a dimensionless time step of $10^{-4}$ were adopted.

As performed in the validation of the numerical scheme, the results are obtained in the dimensionless form and, after, applies an inverse transformation to obtain the results of the interest variables in the dimensional form.

In this work, numerical simulations are conducted to analyze the thermal responses of three different materials that have been widely applied in the manufacture of nanofilms. The materials studied were aluminum, silicon and gold. Such materials present different thermal diffusivities, with gold being the highest and aluminum with the lowest thermal diffusivity. Nanofilms of 0.2 μm width are considered and their initial temperatures are assumed to be 300 K. The physical properties used in the simulations are shown in Table 1.

Table 1**:** Physical properties of materials at 300 K. (Guo and Huo, 2010; Bergman et al., 2007; Cottrell, 1964).

| Material | ρ (kg/m$^3$) | k (W/m·K) | C (J/kg·K) | α·10$^{-6}$ (m$^2$/s) | φ |
|---|---|---|---|---|---|
| Al | 2702 | 237 | 903 | 97.1 | 2.17 |
| Si | 2330 | 163 | 657 | 106.4 | 1.96 |
| Au | 19300 | 317 | 129 | 127 | 3.03 |

Concerning the two different laser pulses applied on the left boundary, one of them presents a Gaussian distribution function (Qiu and Tien, 1992; Tzou, 1995; Zhou and Ma, 2011; Wang et al., 2011; Zou et al., 2014), while the other one presents a Cosseinodal pulse function (Guo and Huo, 2010; Wang et al., 2010). These two functions are defined according to Eqs. (25)-(26)

$$q_G(0,t)=\begin{cases} q_A\times\exp\left(-4\ln(2)\times\left(\dfrac{t}{t_d}\right)^2\right), & t<t_d \\ 0, & t\geq t_d \end{cases} \quad (25)$$

$$q_{Cos}(0,t)=\begin{cases} q_A\times\dfrac{1}{2}\left(1-\cos\left(\dfrac{2\pi t}{t_d}\right)\right), & t<t_d \\ 0, & t\geq t_d \end{cases} \quad (26)$$

where $q_A$ is the laser intensity and $t_d$ is the laser pulse duration time, whose values are assumed to be $5\text{x}10^{11}\text{W/m}^2$ and 10 ps, respectively.

Figure 3 shows a schematic diagram of two different pulse lasers functions. Despite the fact that the two different laser pulses have equal maximum intensity and equal application time, the total energy quantity provided by these two pulse lasers are slightly different, being $q_{Cos}=0.957175\times q_G$.

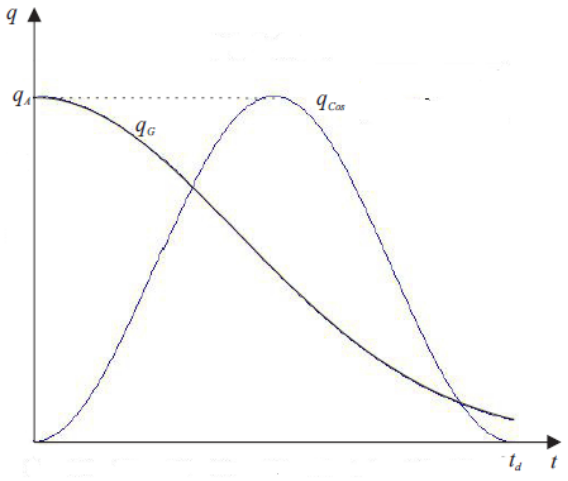


Figure 3. Schematic diagram of two different pulse lasers functions.

The total simulation time for each material has been considered as the time required to the right boundary of the nanofilms suffers a thermal disturbance, i.e., its initial local temperature is changed.

Results are presented separately for each case containing the thermal responses predicted by the Thermomass model for the two different laser pulses. Figures 4, 5 and 6 show the temperature responses at different periods of time for aluminum, silicon and gold nanofilms, respectively.

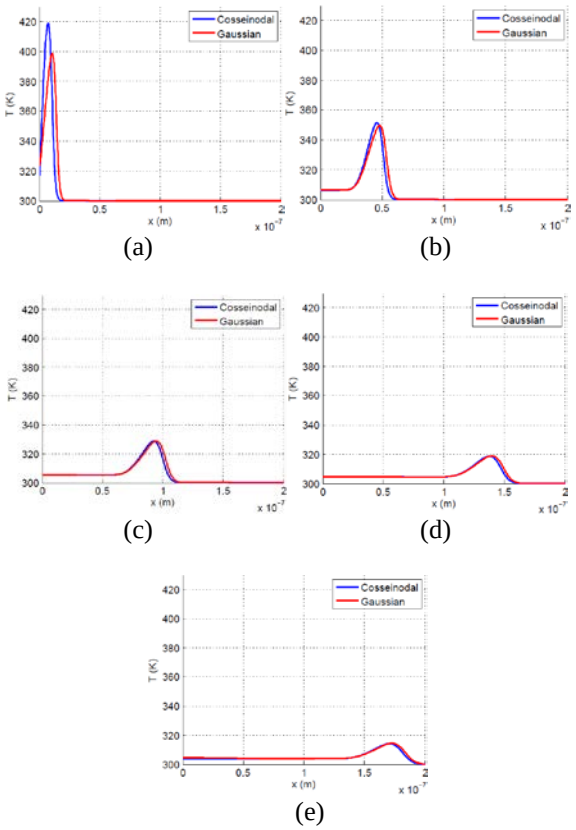


Figure 4. Temperature response in aluminum nanofilm predicted by thermomass model: (a) 10 ps; (b) 40 ps; (c) 80 ps; (d) 120 ps; (e) 150 ps.

Figure 4 shows that during the application of the laser pulses, 10 ps, only points near the left boundary are affected by the thermal disturbances. It is noted also that for the same time the Cosseinodal function has a temperature peak higher than the Gaussian function. However, points that are more distant of the left boundary are more affected by Gaussian function than by the Cosseinodal function. It was found that for later times the temperature peaks tend to be practically equal. This occurs due to the natural tendency that the medium has to attenuate the heat transport. Table 2 shows the total simulation time for the aluminum.

Table 2: Total simulation time for the aluminum.

| Pulse laser | Total simulation time (ps) |
|---|---|
| **Gaussian** | 146.05 |
| **Cosseinodal** | 148.07 |

It was observed that for the two different laser pulses, the difference between the total simulation times is very small, less than 2%. This difference is considered inexpressive. Due to the different total simulation times for the two functions, Fig. 4(e) was plotted for a time step slightly superior to the higher value, i.e., 150 ps.

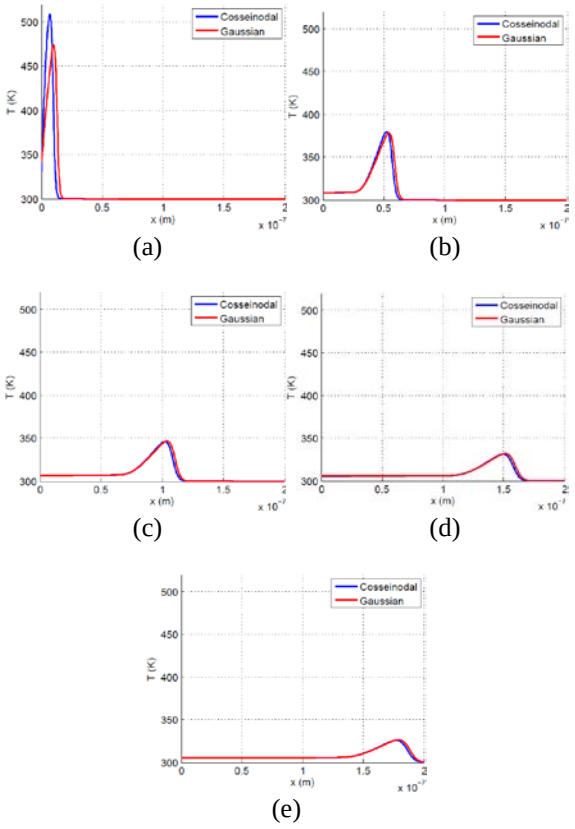


Figure 5. Temperature response in silicon nanofilm predicted by thermomass model: (a) 10 ps; (b) 50 ps; (c) 100 ps; (d) 150 ps; (e) 180 ps.

Figure 5 shows that the heat propagation in the silicon presents the same characteristics observed in the aluminum nanofilm. However, during the laser pulse application time the silicon presented a temperature peak higher than the aluminum. Accordingly to the Thermomass theory, the characteristic time parameter is the time necessary to establish a heat flux (Thermomass gas flow) immediately after a temperature gradient (driven force) be imposed to the medium. It is also directly proportional to the thermal diffusivity of the medium, as expressed by Eq. (15). As can be noticed in Tab. 1, the thermal diffusivity of the silicon is higher than that of the aluminum. Therefore, if these two materials are submitted to the same heating process, it is expected that the silicon has a characteristic time higher than the aluminum, i.e., its total simulation time be higher. As the silicon has a characteristic time higher than aluminum, the energy absorbed by the silicon is also higher. Thus, it is expected that for the laser pulse duration time the silicon presented a temperature peak higher than the aluminum. Table 3 shows the total simulation time for the silicon.

Table 3: Total simulation time for the silicon.

| Pulse laser | Total simulation time (ps) |
|---|---|
| **Gaussian** | 173.43 |
| **Cosseinodal** | 175.38 |

As in the aluminum, it was verified that in the silicon the difference between the simulation times for the two different laser pulses is very small, less than 2%. This difference is also considered inexpressive. Due to the different total simulation times for the two functions, Fig. 5(e) was plotted for a time step slightly superior to the higher value, i.e., 180 ps.

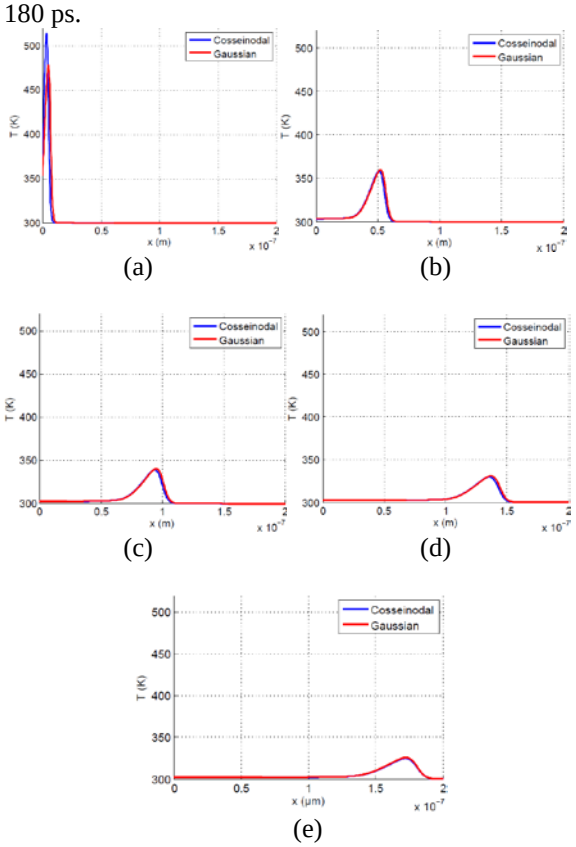


Figure 6. Temperature response in gold nanofilm predicted by thermomass model: (a) 10 ps; (b) 90 ps; (c) 170 ps; (d) 250 ps; (e) 325 ps.

Figure 6 shows thermal responses of the gold nanofilm provided by the Thermomass model for the two laser pulses. As in the silicon, the heat propagation in the gold presented the same characteristics of the aluminum. It is verified that the gold is the material with the highest temperature peak during application of the two laser pulses, 10 ps. In the present work, the gold is the material with the highest thermal diffusivity, according to Tab.1. Therefore, it is expected that this material has the highest temperature peak for the laser pulse duration time and also has the highest characteristic time, i.e., the highest total simulation time. Table 4 shows the total simulation time for the gold.

Table 4: Total simulation time for the gold.

| Pulse laser | Total simulation time (ps) |
|---|---|
| **Gaussian** | 318.81 |
| **Cosseinodal** | 321.20 |

As in the other materials, it was verified that in the gold the difference between the simulation times for the two different laser pulses is very small, less than 2%. This difference is considered inexpressive. Due to the different total simulation times for the two functions, Fig. 6(e) was plotted for a time step slightly superior to the higher value, i.e., 325 ps.

It is verified from the Figures 4-6 that in the laser pulse duration time the materials with higher thermal diffusivities presented higher temperature peaks. However, these materials presented higher total simulation times. Table 5 shows the total simulation time for all materials.

Table 5: Total simulation time for all materials.

| Material | Total simulation time (ps) |
|---|---|
| **Al** | 150 |
| **Si** | 180 |
| **Au** | 325 |

From Tab. 5 is verified that the materials with the higher thermal diffusivities present the higher total simulation times. Due to the different total simulation times for the two functions, Tab. 5 shows total simulation times slightly superior to the higher values.

## CONCLUSIONS

In this work, a numerical study was conducted to evaluate the thermal responses of the transient heat conduction process in nanofilms based on the Thermomass theory. The heat transfer process was assumed unidimensional once that the laser pulse was applied uniformly at the whole left boundary. For the numerical resolution of governing equations it was used the explicit TVD method.

The results were presented in the dimensional form to allow the evaluation of thermal responses caused in different materials by the two laser pulses. The Thermomass theory predicted a heterogeneous temperature distribution with elevated temperature peaks. It was verified during the application of the laser pulses that only points near the thermal disturbance are affected. It was noted that for the same time the Cosseinodal function has a temperature peak higher than the Gaussian function. However, points located far from the left boundary have their temperatures more affected by the Gaussian function than by the Cosseinodal function. For later times, the temperature peaks tend to be practically equal. This is due to the natural tendency that the medium has to attenuate the heat transport. It was also observed that the intensity temporal variation of the two heat sources used in the present work does not influence the heat propagation mode along the nanofilm, independently of the material to be considered. The understanding of as the heat conduction process occurs in nanoscale is expected to be of great importance for improvement and development of the

nanotechnology. Therefore, Thermomass theory is a new concept to investigate the heat conduction process in nanoscale, the thermal responses obtained from this model may prevent the thermal damage caused by technologies of the processing and manufacturing of elements based on high-power laser applications.

## ACKNOWLEDGEMENTS

The authors wish to thank the Brazilian research funding agency CAPES for its support to this work.

## REFERENCES

Bai, C., and Lavine, A. S., 1995, On Hyperbolic Heat-Conduction and the Second Law of Thermodynamics, Journal of Heat Transfer-Transactions of the ASME, Vol. 117, No. 2, pp. 256-263.

Bergman, T. L., Lavine, A. S., Incropera, F. P., and DeWitt, D. P., 2007, *Fundamentals of Heat and Mass Transfer, 6th Edition*, Wiley, New York.

Cattaneo, C., 1948, Sulla Conduzione del Calore, Atti del Seminario Matematico e Fisico della Università di Modena, Vol. 3, pp. 83-101.

Chang, C. W., Okawa, D., Garcia, H., Majumdar, A., and Zettl, A., 2008, Breakdown of Fourier's Law in Nanotube Thermal Conductors, Physical Review Letters, Vol. 101, pp. 075903.

Chen, G., 2000, Particularities of Heat Conduction in Nanostructures, Journal of Nanoparticle Research, Vol. 2, pp. 199-204.

Chen, G., 2005, *Nanoscale Energy Transport and Conversion: a Parallel Treatment of Electrons, Molecules, Phonons, and Photons*, Oxford University Press, New York.

Cottrell, A. H., 1964, *The Mechanical Properties of Matter*, Wiley, New York.

Eesley, G. L., 1990, Picosecond Dynamics of Thermal and Acoustic Transport in Metal Films, International Journal of Thermophysics, Vol. 11, pp. 811-817.

Einstein, A., Lorentz, H. A., Minkowski, H., and Weyl, H., 1952, *The Principle of Relativity*, Dover Publications, New York.

Escobar, R. A., Ghai, S. S., Jhon, M. S., and Amon, C. H., 2006, Multi-Length and Time Scale Thermal Transport using the Lattice Boltzmann Method with Application to Electronics Cooling, International Journal of Heat Mass Transfer, Vol. 49, pp. 97-107.

Fichera, G., 1992, Is The Fourier Theory of Heat Propagation Paradoxical?, in: *Rendiconti del Circolo Matematico di Palermo*, Serie II. Tomo XLI, pp. 5-28.

Fourier, J. B. J., 1878, The Analytical Theory of Heat, Translated, with Notes by Alexander Freeman, M. A., Cambridge: At the University Press.

Guo, Z. Y. and Hou, Q. W., 2010, Thermal Wave Based on the Thermomass Model, Journal of Heat Transfer, Vol. 132, pp. 072403-072403.

Guo, Z. Y., Wang, M., and Yang, N., 2011, Non-Fourier Heat Conductions in Nanomaterials, Journal of Applied Physics, Vol. 110, pp. 064310.

Hua, Y. C., and Cao B. Y., 2014, Phonon Ballistic-Diffusive Heat Conduction in Silicon Nanofilms by Monte Carlo Simulations, International Journal of Heat and Mass Transfer, Vol. 78, pp. 755-759.

Korner, C., and Bergmann, H. W., 1998, The Physical Defects of the Hyperbolic Heat Conduction Equation, Applied Physics a-Materials Science & Processing, Vol. 67, No. 4, pp. 397-401.

Lobão, D. C., 1992, High Resolution Schemes Applied to the Euler Equations, Doctoral Thesis, University of Bristol, UK.

Lobão, D. C., 2002, Microsatellite Thermal Effect by Hyperbolic Heat Conduction, in: *International Symposium on Space Technology*, Matsue-Japan.

Miklos, A., and Lorincz, A., 1988, Transient Thermoreflectance of thin Metal Films in the Picosecond Regime, Journal of Applied Physics, Vol. 63, pp. 2391-2395.

Qiu, T. Q., and Tien, C. L., 1992, Short-Pulse Laser Heating on Metals, International Journal of Heat and Mass Transfer, Vol. 35, No. 3, pp. 719-726.

Terris, D., Joulain, K., Lacroix, D., and Lemonnier D., 2007, Numerical Simulation of Transient Phonon Heat Transfer in Silicon Nanowires and Nanofilms, Journal of Physics: Conference Series Vol. 92, pp. 012077.

Tzou, D. Y., 1995, The Generalized Lagging Response in Small-Scale and High-Rate Heating, International Journal of Heat and Mass Transfer, Vol. 38, No. 17, pp. 3231-3240.

Vernotte, P., 1958, Paradoxes in the Continuous Theory of the Heat Equation, Compute Rendus, Vol. 246, pp. 3154-3155.

Wang, H. D., Ma, W. G., Zhang, X., Wang, W., and Guo, Z. Y., 2011, Theoretical and Experimental Study on the Heat Transport in Metallic Nanofilms Heated by Ultra-Short Pulsed Laser, International Journal of Heat and Mass Transfer, Vol. 54, pp. 967-974.

Wang, H., Liu, J, Guo, Z., and Takahashi, K., 2012, Non-Fourier Heat Conduction Study for Steady States in Metallic Nanofilms, Chinese Science Bulletin, Vol.57, No. 24, pp. 466-479.

Wang, M., Cao, B. Y., and Guo, Z. Y., 2010, General Heat Conduction Equations Based on the Thermomass Theory, Frontiers in Heat and Mass Transfer, Vol. 1, pp. 013004.

Yang, N., Zhang, G., and Li, B., 2010, Violation of Fourier's Law and Anomalous Heat Diffusion in Silicon Nanowires, Nano Today, Vol. 5, pp. 85-90.

Yee, H. C., 1987, Construction of Explicit and Implicit Symmetric TVD Schemes and Their Applications, Journal of Computational Physics, Vol.

68, Issue 1, pp. 151-179.

Zhou, Z., and Ma, Z., 2011, Investigation of Thermomechanical Responses in Ultrafast Laser Heating of Metal Nanofilms, Thin Solid Films, Vol. 519, pp. 7940-7946.

Zou, Y., Cai, J., Huai, X., Xin, F., and Guo, Z., 2014, Molecular Dynamics Simulation of Heat Conduction in Si Nano-Films Induced by Ultrafast Laser Heating, Thin Solid Films, Vol. 558, pp. 455-461.